

Poloidal currents in COMPASS vacuum vessel during symmetrical disruptions: diamagnetic measurements and comparison with analytics

V. V. Yanovskiy¹, V. D. Pustovitov^{2,3}, E. Matveeva^{1,4}, J. Havlicek¹, A. Havranek¹,
J. Hromadka¹, M. Hron¹, N. Isernia⁵, M. Komm¹, O. Kovanda¹, K. Kovarik¹, J. Krbec¹,
T. Markovic¹, R. Panek¹, J. Seidl¹, D. Tskhakaya¹, F. Villone⁵, V. Weinzettl¹

and the COMPASS team

¹*Institute of Plasma Physics of the CAS, Prague, Czech Republic*

²*National Research Centre Kurchatov Institute, Moscow, Russia*

³*Moscow Institute of Physics and Technology, Dolgoprudny, Russia*

⁴*Charles University, Faculty of Mathematics and Physics, Prague, Czech Republic*

⁵*Consorzio CREATE, DIETI, Università degli Studi di Napoli Federico II, Italy*

1. Introduction. For the first time diamagnetic measurements were used to calculate poloidal current induced in the vacuum vessel ('wall') of the COMPASS tokamak during thermal (TQ) and current (CQ) quenches as it was recently proposed in [1]. The results are in good quantitative agreement with both: local measurements of the poloidal current and recent analytical predictions [2].

2. The diagnostic technique. The COMPASS tokamak has 3x24 sensors for measuring the toroidal magnetic field B_ζ (toroidal Mirnov coils, TMCs) in three different toroidal locations [3], see Fig. 1. This unique set of diagnostics allows to deduce the poloidal and toroidal distributions of poloidal current i_w in the vessel by using the Ampere's law as $\mu_0 i_w = 2\pi R \Delta B_\zeta$, Eq. (1) in [3]. The fundamental harmonic of i_w must be the poloidal eddy current I_w . We can separate it and compare the result with I_w extracted from diamagnetic measurements. The higher harmonics in the TMC signals are interpreted as indications of the halo currents flowing from plasma to the wall and then back to the plasma.

3. The data. For the downward VDE shown in Figs. 2 and 3, the poloidal current i_w is larger at the bottom part of the vessel than that in the upper part, as is illustrated in Fig. 4 with numerically integrated signals from TMCs 8 (top) and 18 (bottom). These give $i_w(18)$ almost three times larger than $i_w(8)$, a clear evidence of halo currents at the bottom. For downward VDEs the upper coils '8' are far from the plasma column shrinking at the bottom, therefore they measure primarily the eddy current. In Fig. 5a, the eddy current measured by these coils

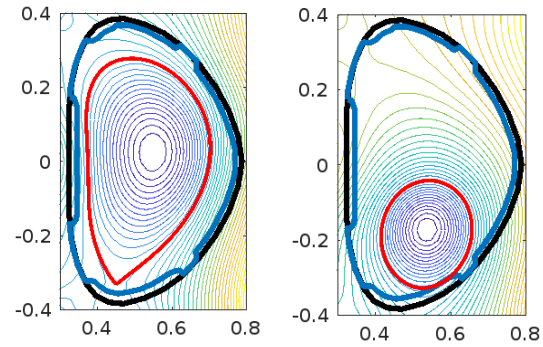
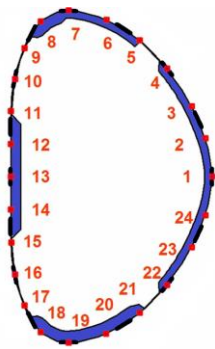
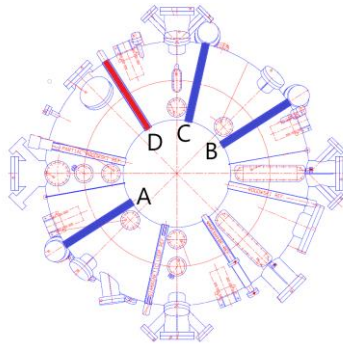


Fig. 1. (a) Top view of the VV with indicated positions of the diamagnetic loop 'D' (0°) and three poloidal arrays of TMCs: 'A' (+90°), 'B' (-90°) and 'C' (-45°), (b) poloidal cross-section of the VV with positions of TMCs, from 1 to 24, first wall is shown by blue.

Fig. 2. EFIT reconstruction of the shot #18770: (a) at the beginning of downward VDE (1150 ms), (b) at the beginning of CQ (1151.25 ms). Vessel is shown by black colour, first wall by blue, and LCFS by red.

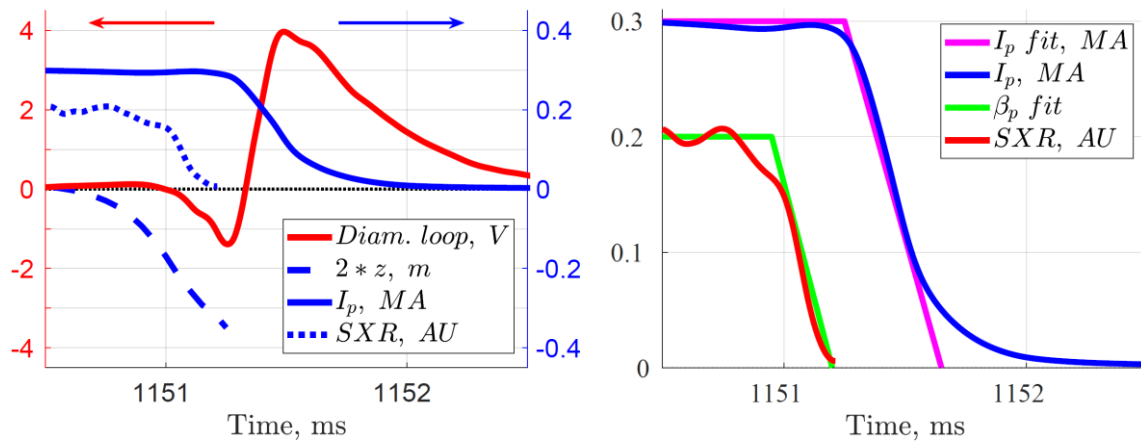


Fig. 3. (a) Diamagnetic signal V , vertical plasma position z , plasma current I_p , and SXR intensity during an intentional downward VDE for shot #18770, (b) linear fit of I_p and β_p for comparison with analytics.

is compared with current deduced from diamagnetic measurements using formula (36) from [1]: $I_w = V / R_w$, where I_w is the poloidal current in the wall, V is the measured voltage and $R_w = 0.22 \text{ m}\Omega$ is the poloidal resistance of the wall. It is important to notice, that the above formula is valid only for the (ITER-like) diamagnetic loop mounted on the wall, which is the case for COMPASS, see Fig.6 [4]. One can see good quantitative agreement both for TQ, within 22% (-6 kA for DT vs. -6 kA, -6 kA and -7.3 kA for TMCs 'A', 'B' and 'C', respectively), and CQ, within 24% (18 kA for DT vs. 14.5 kA, 15.5 kA and 16.5 kA for TMCs 'A', 'B' and 'C', respectively). The numerically integrated signal from TMCs does not decay to zero, which is the diagnostic error. The time shift of 0.1 ms between currents deduced from the probe and diamagnetic measurements comes probably from the shielding of TMCs by 0.25 mm thick Inconel covers.

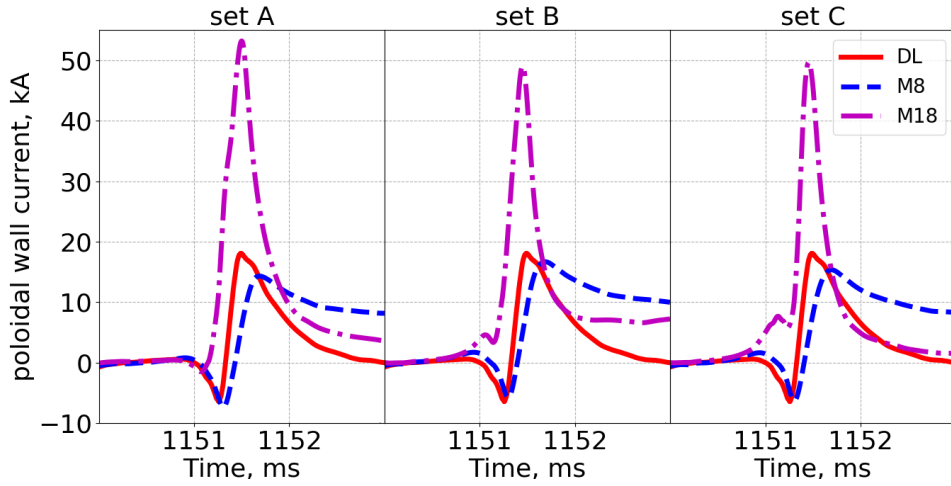


Fig. 4. Poloidal wall current deduced from diamagnetic signal (red solid line) and TMCs ‘8’ (blue dashed) and ‘18’ (magenta dash-dotted) in toroidal locations A, B and C during downward VDE from shot #18770.

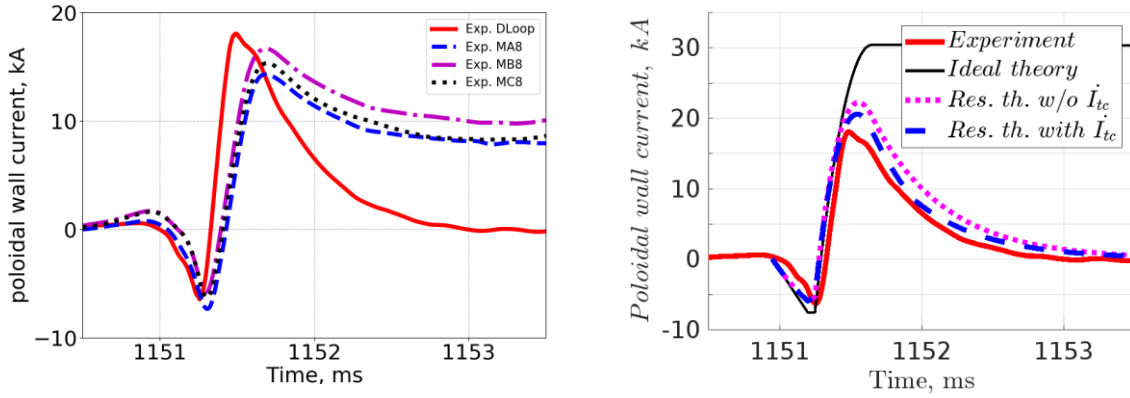


Fig. 5. Poloidal wall current deduced from diamagnetic signal (red solid) and: (a) from TMCs ‘8’ in toroidal locations A (blue dashed), B (magenta dash-dotted) and C (black dotted); (b) from analytical modelling using Eq. (1) for the ideal case (black solid) and for the resistive cases with (blue dashed) and without (magenta dotted) the account of current change in toroidal coils.

4. Comparison with analytical predictions. For this purpose we use Eq. (24) from [2],

$$L_w \frac{dI_w}{dt} + R_w I_w + \frac{d}{dt} (\Phi_{pl} - \Phi_{pl}^0) + L_w \frac{dI_{tc}}{dt} = 0, \quad (1)$$

and approximate TQ and CQ by a linear fit, as illustrated in Fig. 3b. During 0.25 ms, the TQ lasting from 1150.95 ms till 1151.20 ms brings the pre-disruption value $\beta_p = 0.2$ to zero. At 1151.25 ms, the 0.4 ms long CQ starts with full current drop from 0.3 MA. The linear quench times $\tau_{iq} = 0.25$ ms and $\tau_{cq} = 0.4$ ms are comparable with $\tau_1 \equiv L_w / R_w = 0.5$ ms, the resistive time of the COMPASS vessel ($L_w = 0.11$ μ H is its poloidal inductance). In Eq. (1), I_{tc} is the full poloidal current in the toroidal coils and

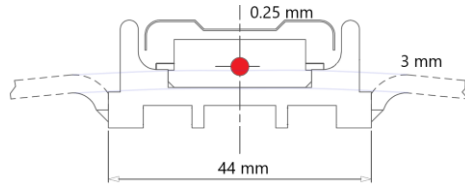


Fig.6. Part of the toroidal cross-section on HFS with diamagnetic loop (red dot). The VV is shown by dashed lines. The loop is protected by 0.25 mm Inconel 625 cover. Semi-transparent blue lines indicate the average radius of the VV.

$$\Phi_{pl} - \Phi_{pl}^0 \approx \frac{2K}{K^2 + 1} \frac{(\mu_0 J_{pl})^2}{8\pi B_0} (1 - \beta_p), \quad (2)$$

where $K = 1.8$ is the plasma vertical elongation, $B_0 = 1.15$ T is the toroidal magnetic field, $J_{pl} = 0.3$ MA and $\beta_p = 0.2$ are the pre-disruption net plasma current and the poloidal beta.

Results for the ideal wall, i.e. without second and forth terms in (1), are shown in Fig 5b by black solid line. Minimum current for TQ with $\tau_{iq} / \tau_1 = 1/2$ is $I_w^{iq} = -7.6$ kA, only 21% lower than the value of -6.3 kA deduced by diamagnetic technique. Maximum current for CQ with $\tau_{cq} / \tau_1 = 4/5$ is $I_w^{cq} = 30.4$ kA, 69% higher than the measured value of 18 kA.

The toroidal coil current $I_{tc} \approx 3.2$ MA has been ramped-up quasi linearly by 0.16% (from 49.98 kA to 49.06 kA per turn) in the interval between 1151.25 ms (start of CQ) and 1151.95 ms. For 16×4 turns this corresponds to $\Delta I_{tc} = 5.1$ kA in $\Delta t = 0.7$ ms. Results for the resistive wall with and without the last term in Eq. (1) are presented in Fig. 5b, by dashed and dotted lines, respectively. For TQ $I_w^{iq} = -6.0$ kA, just 5% different from the measured value. During CQ the current reaches 22.2 kA for the simplified case without change of I_{tc} , and slightly more accurate value of 20.5 kA if all terms are taken into account. In the last case the analytical estimate is only 14 % higher than the experimental value deduced from DT and 41% higher than the value of 14.5 kA, based on the signal from TMC A8, see Figs. 5a and 5b.

5. Conclusions. Results show good quantitative agreement of I_w obtained by diamagnetic technique with local measurements and analytical predictions. The next step will be to validate the experimental and analytical results against the CarMa0NL code [5].

[1] Pustovitov V D 2019 Fusion Eng. Des. 138 53-58

[2] Pustovitov V D 2017 Fusion Eng. Des. 117 1-7

[3] Knight P J et al 2000 Nucl. Fusion 40 325

[4] Dubrov M L and Pustovitov V D 2019 Plasma Phys. Control. Fusion 61 065018

[5] Villone F et al 2013 Plasma Phys. Control. Fusion 55 095008